GEOMORPHOLOGY OF THE NORTHEAST PLANNING AREA, NATIONAL PETROLEUM RESERVE–ALASKA, 2004

FOURTH ANNUAL REPORT

Prepared for

ConocoPhillips Alaska, Inc.
P.O. Box 100360
Anchorage, AK 99510

and

Anadarko Petroleum Corporation
3201 C Street, Suite 603
Anchorage, AK 99503

Prepared by

M. Torre Jorgenson
Dorte Dissing

ABR, Inc.—Environmental Research & Services
PO Box 80410
Fairbanks, AK 99708

and

Yuri L. Shur
Matt Bray

Department of Civil Engineering
University of Alaska
PO Box 755900
Fairbanks, AK 99775

February 2005

TABLE OF CONTENTS

LIST OF FIGURES

ACKNOWLEDGMENTS

This study was funded by ConocoPhillips Alaska, Inc., and managed by Caryn Rea, Environmental Studies Coordinator. Jason Garmin, science teacher, Trapper School, and Olivia Cabinboy, Nanuk Corporation helped coordinate student participation in the arctic coastal dynamics workshop. Dorte Dissing help with GIS production and Sue Bishop technically reviewed the report, and Pam Odom helped with report production.

INTRODUCTION

Permafrost development on the Arctic Coastal Plain in northern Alaska greatly affects the engineering properties of the soil (Johnson 1981, Kreig and Reger 1982, McFadden and Bennet 1991), the ecological conditions at the ground surface (Billings and Peterson 1980, Webber et al. 1980, Walker 1981), and the response of the terrain to human activities (Brown and Grave 1979, Webber and Ives 1978, Lawson 1986). Of particular interest for assessing potential impacts from oil development in the National Petroleum Reserve–Alaska (NPRA) are: (1) identifying terrain relationships for predicting the nature and distribution of ground ice across the landscape; and (2) predicting the responses of permafrost to disturbance.

During a multiyear effort to address these issues, we initially focused on characterizing and mapping terrain units on the coastal plain (Jorgenson et al. 2002, Jorgenson et al. 2003) and assessing landscape change (shoreline erosion and lake-basin development). Substantial effort was directed to assessing the varying nature and abundance of ground ice (primarily segregated ice) associated with the terrain units and the implications for terrain sensitivity to disturbance. In 2003, the effort was expanded to include river floodplains and the assessment of changes associated with ice-wedge degradation (Jorgenson et al. 2004). Although these earlier studies highlighted the importance of ice wedges in determining terrain sensitivity, the abundance and distribution of ice-wedges were not quantified because of the high sampling requirements needed to measure ice-wedges dimensions and abundance from cores. To address this data gap, this study was designed to: (1) determine the morphological characteristics of ice wedges; (2) map the distribution of ice wedges on various terrain units to estimate the variability in ice-wedge abundance; and (3) assess the use of ground-penetrating radar GPR for mapping ice wedges.

Although ice wedges have been studied for nearly a century since the pioneering work of Leffingwell (1919), little progress has been made in understanding their nature, abundance, and distribution. The mechanisms of ice-wedge development through thermal contraction cracking have been adequately explained (Leffingwell 1919, Lachenbruch 1962, Mackay 1992), but little is known about variation in ice-wedge characteristics across the arctic landscape. Estimates of the volume of ice wedges near the ground surface have been relatively consistent: 20% at Flaxman Island (Leffingwell 1919), 20% at Barrow (Brown 1968), and 12–16% for the Mackenzie River Delta (Pollard and French 1980), and 0 to 20% on the Colville River Delta depending on terrain unit (Jorgenson et al. 1997). Only the last study addressed the variability of ice wedges across diverse terrain, leaving large gaps in our knowledge.

GPR has long been used in geophysical investigations of permafrost characteristics (Anna and Davis 1976, Arcone et al. 1982, Kovacs and Morey 1985, Pilon et al. 1985, Scott et al. 1990). For permafrost studies, it has been most successful for identifying the upper permafrost boundary because of the distinctive dielectric properties of the thawed active layer over permafrost and the abundant ice that often accumulates at the permafrost table (Arcone and Delaney 1982, Doolittle et al. 1990, Hinkel et al. 2001). GPR has also been useful for determining the locations of ice wedges, but has provided minimal information on the physical characteristics of ice wedges. Because of the large dielectric variability of the surface and the severe ground clutter caused by the short wavelengths used, the image patterns used to identify ice wedges are sometimes masked by reflections from the permafrost table or other material interfaces (Arcone and Delaney 1982, Hinkel et al. 2001, Fortier and Allard 2004). Hoping that technological improvements have overcome some of these limitations, we also evaluated the use of GPR using newer, commercially available equipment with dipole antennas that can be programmed for easy acquisition of survey data along both transects and grids, and newer image-processing software for 3-D imaging.

Better information on ice-wedge characteristics is needed to improve our understanding of the role of massive ice in terrain sensitivity and thermokarst development. While naturally occurring thermokarst is fundamental to ecological processes in arctic lowlands (Britton 1957, Billings and Peterson 1980, Walker et al.

1980, Carter et al. 1987), human-induced thermokarst is a concern for land development in the Arctic because of the subsequent changes in hydrology, soils, and vegetation (Brown and Grave 1979, Jorgenson 1986, Lawson 1986, Walker et al. 1987). In the context of oil development activities, specific concerns include the possibility of thermokarst caused by off-road and seismic-trail disturbances (Walker et al. 1987, Emers and Jorgenson 1997); alteration of drainage patterns following road development, road dust, oil spill cleanups (Jorgenson et al. 1991, Jorgenson et al. 1992); closeout and rehabilitation of reserve pits (Burgess et al. 1999); and gravel removal after site abandonment (Jorgenson and Kidd 1991, Kidd et al. 1997). During the last decade, improved knowledge on ground-ice characteristics and terrain sensitivity have been used to help reduce impacts from seismic exploration (Jorgenson et al. 2004) and ice roads (Pullman et al. 2005), avoid sensitive terrain during facility planning for the Alpine (Parametrix 1997) and NPRA (Entrix 2004) oil developments, and improve designs for land rehabilitation that incorporates thermokarst as a process to create habitat diversity and improve waterbird habitat (Kidd 2004).

Specific objectives of this study were to:

1) describe the morphological characteristics of ground ice in the form of ice wedges as the basis for estimating ice-wedge volumes;
2) evaluate the relationship between ice-wedge abundance and terrain units by mapping the occurrence of ice wedges on various terrain units and calculating ice volumes; and
3) assess the usefulness of ground-penetrating radar for mapping ice-wedge distribution.

METHODS

MORPHOLOGY

The dimensions and characteristics of ice wedges were described at 24 exposures along Fish Creek (Figures 1 and 2). The exposures were first shoveled clear of soil, scraped with a shovel, hoe, and knife to expose fresh ice and soil material, and washed with water. Each exposure was photographed with a graduated soil probe for scale. The exposed ice wedges were then described, including dimensions, ice structure, color, soil and bubble inclusions, and crystal size.

After examining polygonal patterns on the ground surface above the exposures, 12 of the exposures were determined to provide transverse cross-sectional views, while the others were longitudinal sections. Only these wedges were used to calculate ice volumes. For each of these 12 wedges, scale was determined on a computer based on the graduated probe in the photograph. Once the scale was determined, widths were measured at 0.5 m depth intervals. These data were used to determine the mean width (across the group of 12 ice wedges) for each depth increment and the mean width for the top 2 m.

ABUNDANCE AND DISTRIBUTION

The abundance (volume) and distribution of ice wedges were estimated for the nine dominant terrain units based on mapping of ice wedges and estimates of wedge dimensions. The distribution of ice wedges was mapped "on-screen" over a high-resolution (2 ft pixel size) orthophoto mosaic developed from 2001 aerial photography using ArcMap 9 GIS software. The ice wedges were mapped within 3 replicate map areas (1 hectare each), for each of nine terrain units (Figure 1). The occurrences of the dominant terrain units (occupying 75% of area) were obtained from the terrain unit map for the area produced by Jorgenson et al. (2002). The presence of ice wedges was photointerpreted by searching for linear features, paired polygon rims, impounded water in troughs, and differences in color and texture indicative of polygonal troughs and rims. The ice wedges initially were delineated as map polygon (regions) following the centerline of the wedges that comprise each ice-wedge polygon. These map polygons were used to calculate ice-wedge polygon density and size. The map polygons then were converted to line features and trimmed to the 1-ha map area boundaries. The cumulative lengths of lines delineating the ice wedges were summarized for each map area, and the mean cumulative length for the three replicate map areas was calculated for each terrain unit.

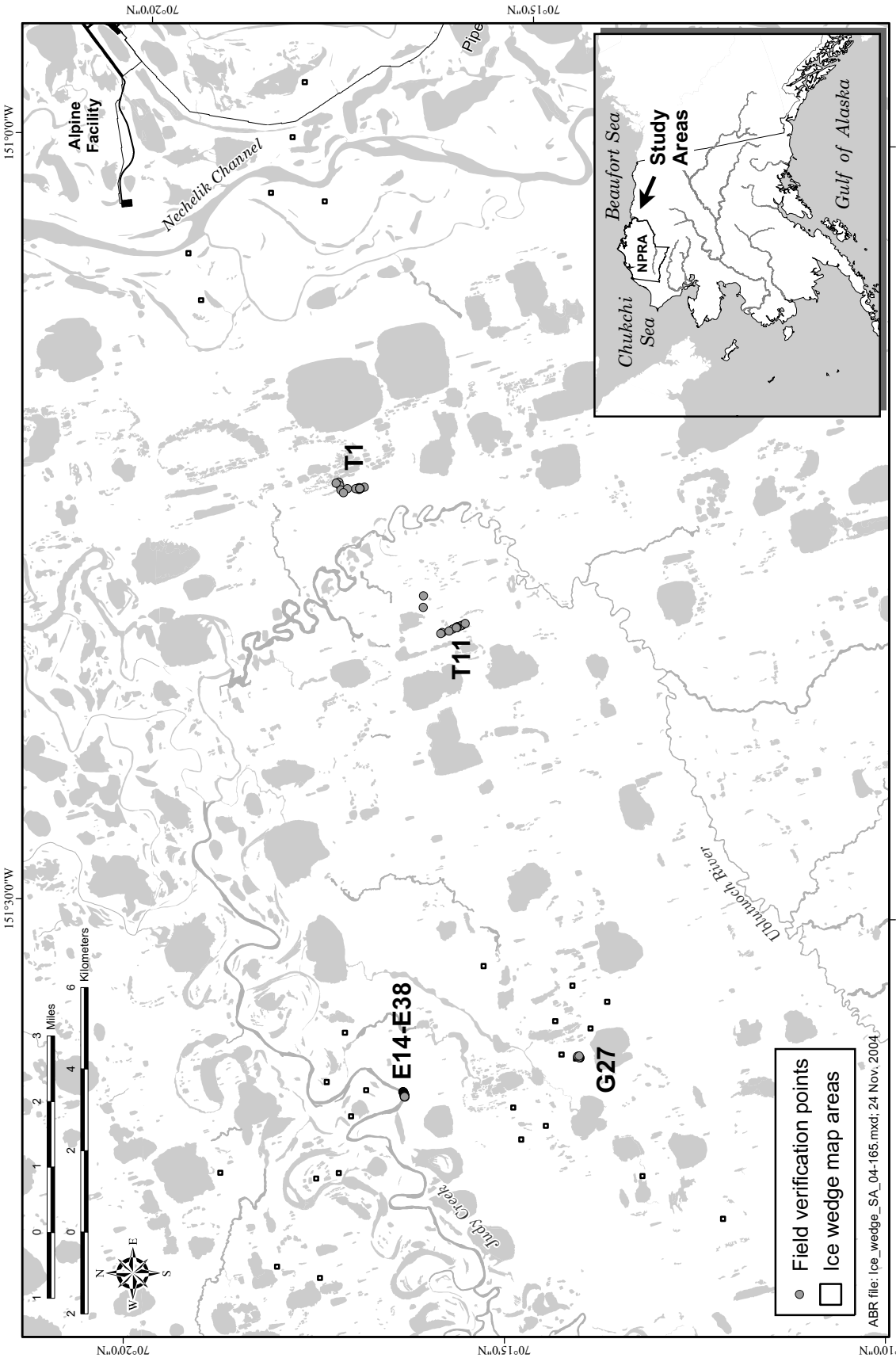

Figure 1. General map showing locations of soil exposure sampling and ground-penetrating radar surveys in the Northeast Planning Area, NPRA, 2004.

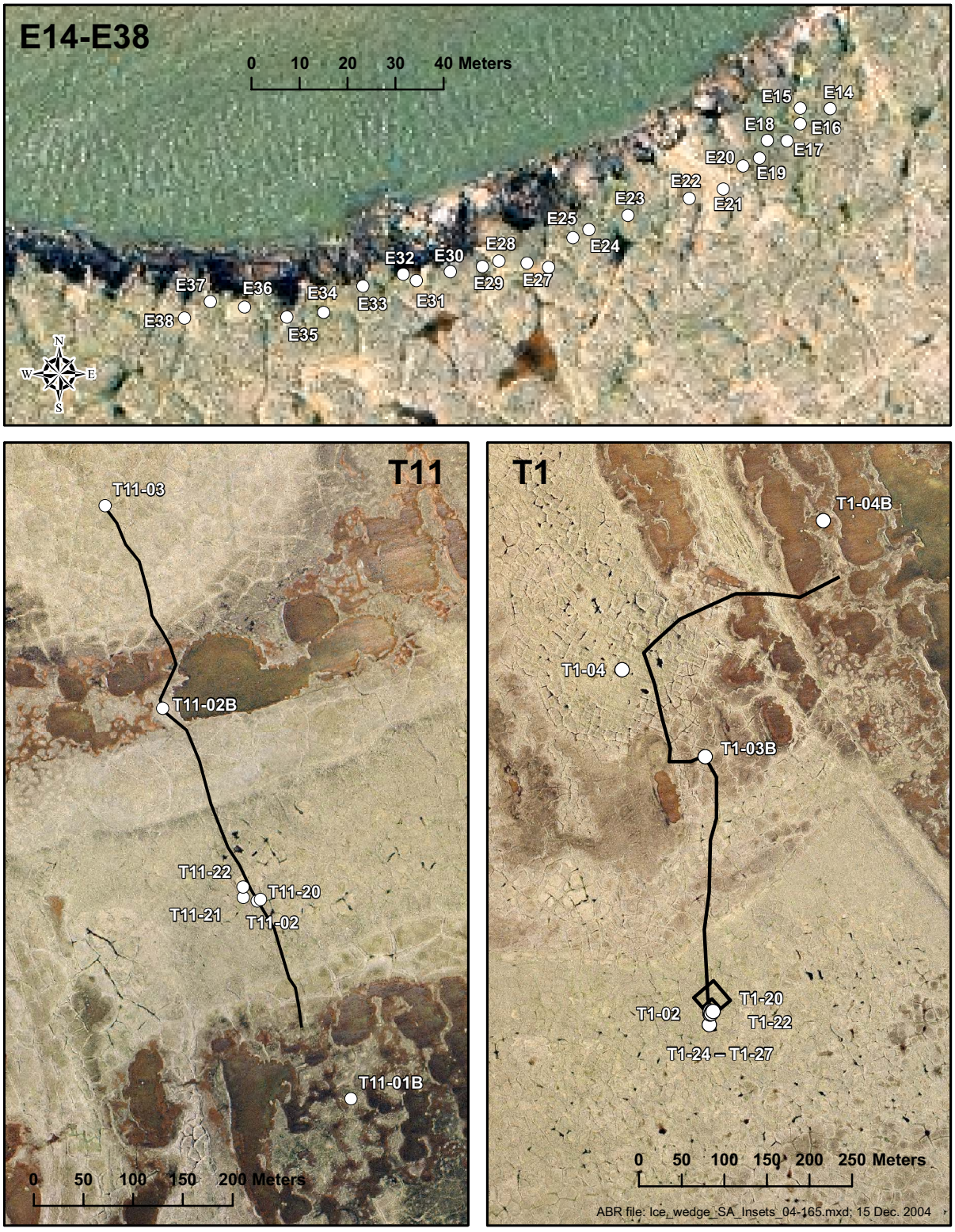

Figure 2. Detailed maps showing locations of soil exposure sampling (top) and ground-penetrating radar surveys at T1 (bottom right) and T11 (bottom left) in the Northeast Planning Area, NPRA, 2004.

The abundance of ice in the top 2 m of permafrost was calculated using the measured cumulative lengths and estimates of ice-wedge dimensions for each terrain unit. We used the measurements of ice-wedge dimensions we obtained for alluvial-marine deposits (1.7 m), but data were not available for the other terrain units because they were topographically lower and good exposures with intact ice wedges were difficult to find. For the other terrain units, we qualitatively estimated the mean width of ice wedges as a function of ice-wedge polygon density. This method of estimation was based on the assumption that the mean size of ice wedges within a terrain unit is related to age (number of cycles for ice-wedge cracking and growth), which in turn is related to ice-wedge density (the smaller the polygon the older the age). The material type was also was a factor, based on the assumption that ice wedges in organic-rich material are larger than those in sandy material. Based on these assumptions, we assigned mean widths of the top 2 m of the ice wedges for eolian sand (1.0 m), delta abandoned overbank (2.0 m), meander abandoned overbank (1.5 m), delta inactive overbank (1.0 m), meander inactive overbank (1.0 m), lacustrine ice-rich center (2.0 m), lacustrine ice-rich margin (1.0 m), and lacustrine ice-poor margin (0.5 m) deposits.

GROUND-PENETRATING RADAR

A ground-penetrating radar (GPR) creates a subsurface image by transmitting a short pulse of electromagnetic (EM) energy into the ground to generate a wave front that propagates downward (Annan and Davis 1976). The amplitude of the EM signal that is reflected back to the surface varies in response to changes in the bulk electrical properties of different subsurface lithologies and the character or abruptness of the interface. A receiver records the amplitude of the reflected energy in relation to the delay time of the energy pulse. The two-way delay time from when it is transmitted to when it is received is a function of EM propagation velocity through the soil and the depth of subsurface reflecting materials. Images are created from the recorded data by plotting the amplitude of the reflected signal (expressed as line thickness or color) by horizontal survey distance and vertical two-way travel time in nanoseconds.

GPR surveys to assess the distribution of soil and ice materials were conducted along transects and within small grids. At sites T1 and T11 (Figure 1), long transects (650 m and 580 m, respectively) were surveyed to assess differences in materials across a range of terrain units. Both a 30-m (2-m line spacing) and a 15-m (1-m line spacing) grid were surveyed on an ice-rich alluvial-marine deposit at site T1 (Figure 2). Data from the grids were used to create 3-dimensional maps of the amplitudes of reflected electromagnetic signals, which respond to differences in soil materials.

The GPR surveys were done using a portable, wheel-mounted, Noggin 250 Smart Cart system manufactured by Sensors and Software, Inc., Mississauga, Ontario. The system uses dipole transducers at 125 and 350 MHz to measure the amplitude of reflected EM signals at time intervals from 5 to 300 ns. Data were digitally recorded for later analysis.

The data were analyzed using EKKO View and EKKO Mapper software from Sensors and Software, Inc. After considerable experimentation with processing parameters, the grid and transect data were plotted using “Dewow” signal filtering, horizontal averaging of 30 traces, and vertical averaging of 5 traces, to remove noise and improve visualization of subsurface patterns.

RESULTS

MORPHOLOGY

DIMENSIONS

Examination of 24 exposed ice wedges along Fish Creek revealed wide variability in both dimensions and ice characteristics (Figure 3). Twelve of the exposed wedges provided transverse cross-sectional views that were useful for measuring width and depth, while the other exposures provided longitudinal views. The mean top width of the 12 wedges where cross sections were exposed was 1.3 m. Mean width increased to a maximum of 1.9 m at 1 m below the wedge top, then gradually decreased to 1.2 m at the 2-m depth and 0.6 m (extrapolated) at the 3-m depth (Figure 4). Many wedges had maximum widths of ~3 m, and the largest wedge had a maximum width

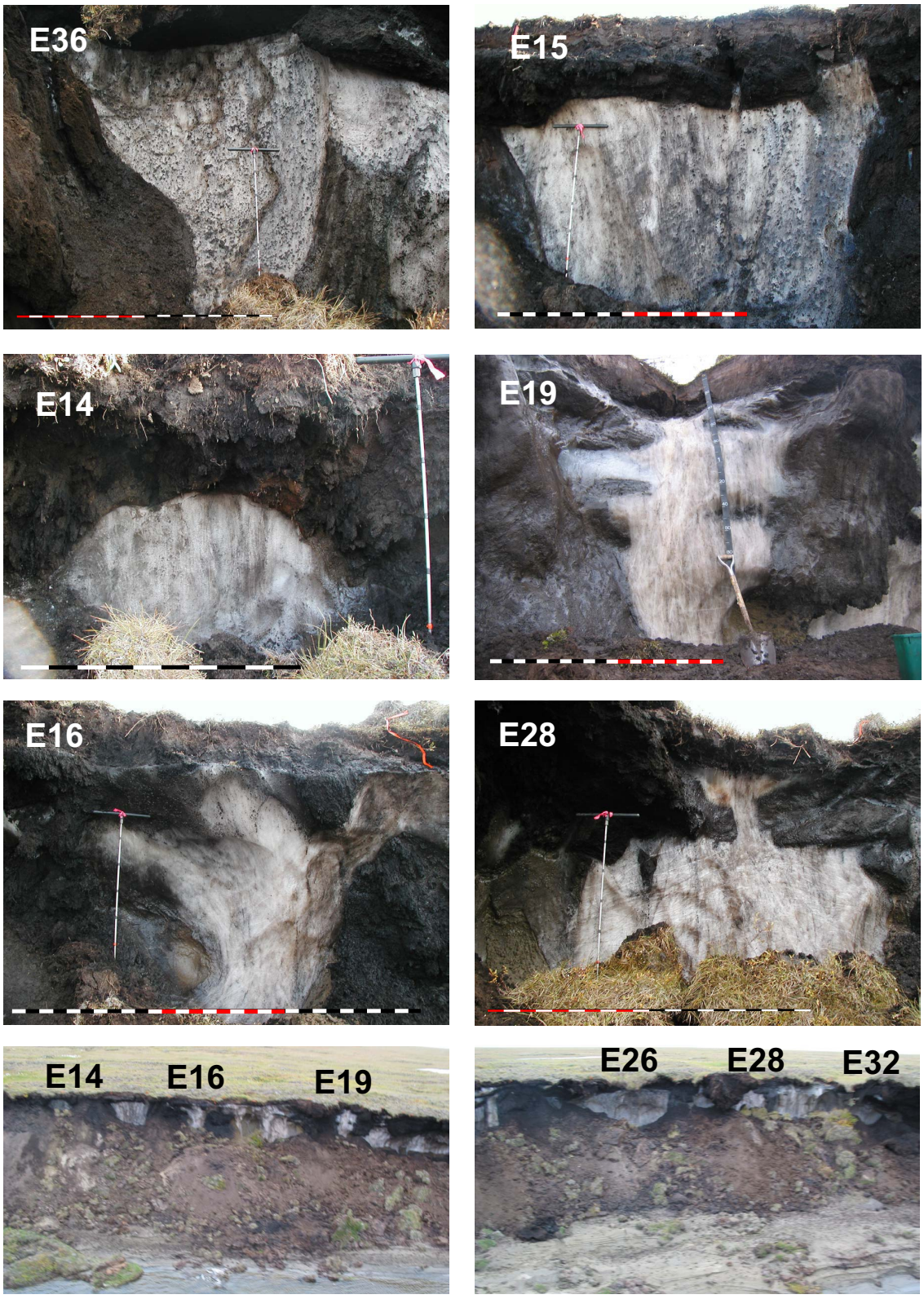

Figure 3. Photographs of exposed ice wedges along Fish Creek in the Northeast Planning Area, NPRA, 2004.

of 5 m. The mean width of the top 2 m, for the group of 12 wedges, was 1.7 m. Bottom depths were rarely obtained, but width trendlines of exposed portions of the wedges indicate wedges usually extended 3–4 m below the top of the wedge. The tops of the wedges generally were 0.3–0.4 m below the ground surface.

Several factors affect the variation in width of ice wedges. First, the width of an ice wedge changes with depth because width is affected by the magnitude of the ground-temperature fluctuations, which are greatest near the ground surface. Consequently, wedge contraction and cracking also are greatest near the surface, creating the distinctive wedge shape (E36 in Figure 4). Below 3–4 m depth, temperature fluctuations usually are insufficient to cause contraction cracking of ice wedges.

Second, soil materials affect ice-wedge contraction and resistance of the soil to deformation from expanding ice wedges. The greater the ice content in the soil the greater the contraction coefficient, so that ice-rich organic material contracts more than ice-poor sand. Similarly, ice-rich organic material is more easily deformed by lateral pressure from the expanding ice wedges than is ice-poor sand or gravel. Therefore, ice wedges typically are much wider in organic material than in sand. This is evident in the exposures where ice-wedge development is highly restricted in the sandy materials (note yellowish sand at bottom of E19 in Figure 4).

Finally, the ice wedges were often narrower at the tops, due to active-layer fluctuations and degradation of the surface of the wedges. When a wedge recovers and regrows during periods of rapid active-layer thinning, the growth is from the center creating a new, thinner wedge above the older degraded surface (E15 in Figure 4). When active-layer recovery and thinning is slower, or when additional organic material accumulates at the surface and raises the active layer upward, a broader center develops as the newly created ice in the center of the cracking wedge accumulates both upward and laterally (E14 in Figure 4).

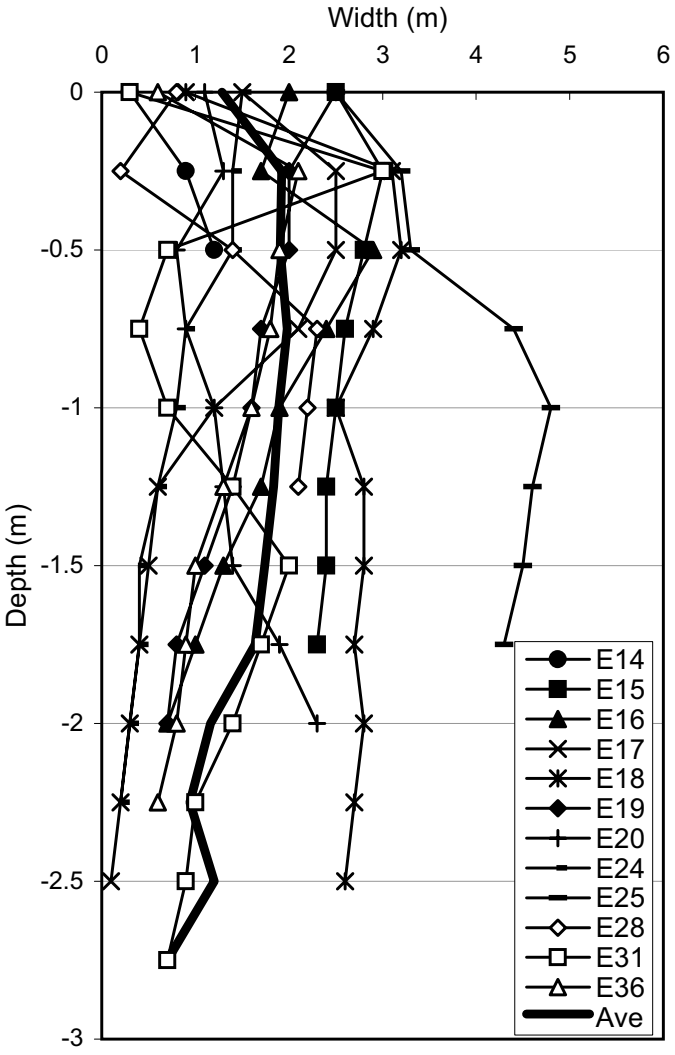

Figure 4. Vertical profiles of the individual and mean widths (end view) of 12 ice wedges along Fish Creek in the Northeast Planning Area, NPRA, 2003.

ICE CHARACTERISTICS

Two distinct types of ice were evident in the wedges. First, "wedge ice" initially formed during ice-wedge development was opaque and had a distinctive, whitish color. Entrained organic and mineral material and small (0.1–0.5 mm) air bubbles were relatively abundant and the cyclic addition of material in the ice gives it a vertically foliated structure. This ice most often was vertically distributed continuously from the permafrost surface as a wedge-shaped mass (E15 and E36 in Figure 4). The wedge ice also was frequently observed, however, at irregular depths

after degradation of the surface or marginal portions of the wedge ice, which often obscured the original wedge shape (E16 and E28 in Figure 4).

The second type of ice is referred to as "congelation ice" because it congeals (freezes) from large, irregular masses of water that have intruded into thawed cavities in wedge ice or soil. This ice is the result of melting caused by flowing surface water or suprapermafrost groundwater, or possibly by irregular deepening associated with impounded water in thermokarst troughs, and the subsequent freezing of the water in the cavity. The ice usually is yellowish-brown in color due to presence of dissolved organic matter (surface ice at E28), lacks stratification or is weakly stratified horizontally, and bubbles are much less abundant. In some cases, the ice is dark brown from abundant organic matter that has frozen within the ice (see horizontal, marginal dark intrusions at E19). The margins of the ice masses are rounded, indicating that the freezing occurred in thawed cavities. Congelation ice was common along the top and upper margins of many of the exposed wedges that we examined. It also occurred near the surface at the margins of large wedges, where it was oriented diagonal or perpendicular to the orientation of the wedge ice. We interpret this ice to have formed in the cavity caused by the cracking of the highly extended "wings" of the wedges due to pressures built up in the adjacent compressed soil (E19). During coring in 2003, we often found congelation ice associated with wedges that were in the advanced stages of stabilization after being partially degraded, as indicated by the presence of sedge vegetation in a subsided trough and the presence of new sedge peat over dead tussocks. The congelation ice, however, was not observed from cores taken from stable, undisturbed wedges found under tussock tundra or barely distinguishable troughs. Although we recognized at the time that the congelation ice was different from wedge ice, we did not adequately differentiate the morphology and genesis of the ice until 2004, when we had the opportunity to examine numerous exposures. Congelation ice appears to be primarily associated with older alluvial-marine deposits, where the wedges are relatively old (more susceptible to degradation over a longer climatic period) and large (more area for degradation). We estimate that the congelation ice contributes about 5–10% of the total volume of massive ice (wedge and congelation ice) in the top 2 m of permafrost in alluvial-marine deposits.

Also of interest when examining the wedges was the deformation of soils by the expansion and contraction of the soil and the displacement of soil by the growing wedges. Some of the prominent features were: (1) folding and uplifting of deeper mineral material toward the surface near the ice wedges, (2) plastic flow of small amounts of surface material downward along the margin of the wedges, (3) squeezing and vertical deformation of soil in a gradient from the wedge to the center ice-wedge polygon, and (4) small fractures with lateral displacement of soil layers near the permafrost table. Much of this deformation probably is caused during the summer when the soil expands outward from the center of the ice-wedge polygons toward the ice wedges and the warmer permafrost temperatures allow more plastic movement.

ABUNDANCE AND DISTRIBUTION

Delineation of the centerlines of ice wedges through interpretation of high-resolution aerial photography revealed large differences among terrain units in the abundance and distribution of ice wedges (Figure 5). Mean area of the polygons formed by the ice-wedge networks was nearly 10-fold larger in delta inactive overbank deposits than in eolian sand or alluvial-marine deposits (Figure 6). Conversely, the density of polygons and the cumulative length of the ice wedges were nearly 10-fold higher in the eolian sand and alluvial-marine deposits than in the ice-poor margins of recently drained lake basins. Thus, the smaller the ice-wedge polygons, the greater their density, and the greater the cumulative length of ice wedges.

There also were large differences among terrain units in the estimated volumes of wedge ice, although the data are less definitive due to the lack of information on ice-wedge dimensions for some terrain units. Based on quantitative measurements of ice-wedge dimensions from alluvial-marine deposits, and on the estimated ice-wedge dimensions for the other deposits (see *Dimensions*, above), the volume of wedge ice in the top 2 m of

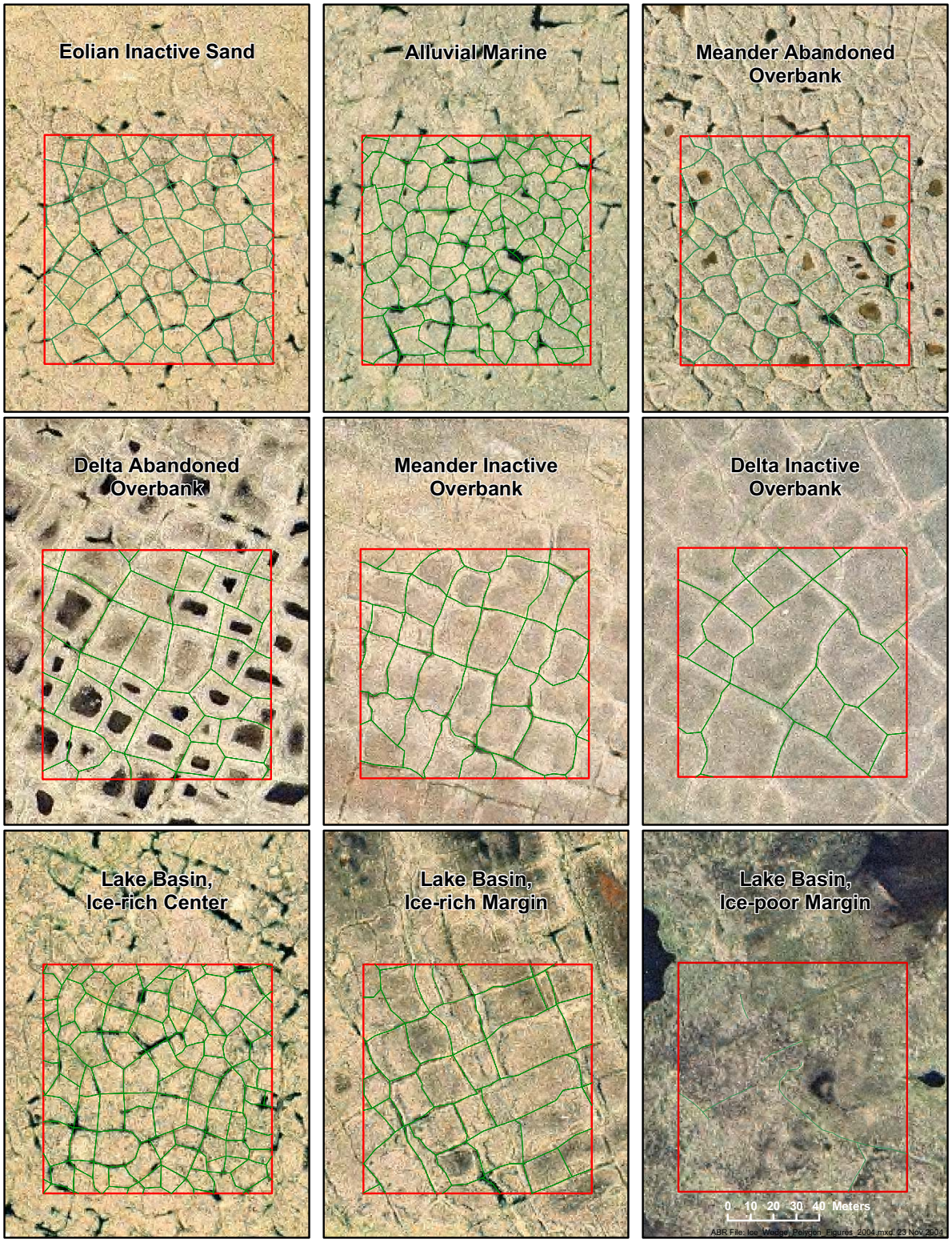

Figure 5. Representative maps of ice-wedge distributions (wedge centerlines) for nine geomorphic units in the Northeast Planning Area, NPRA, 2003.

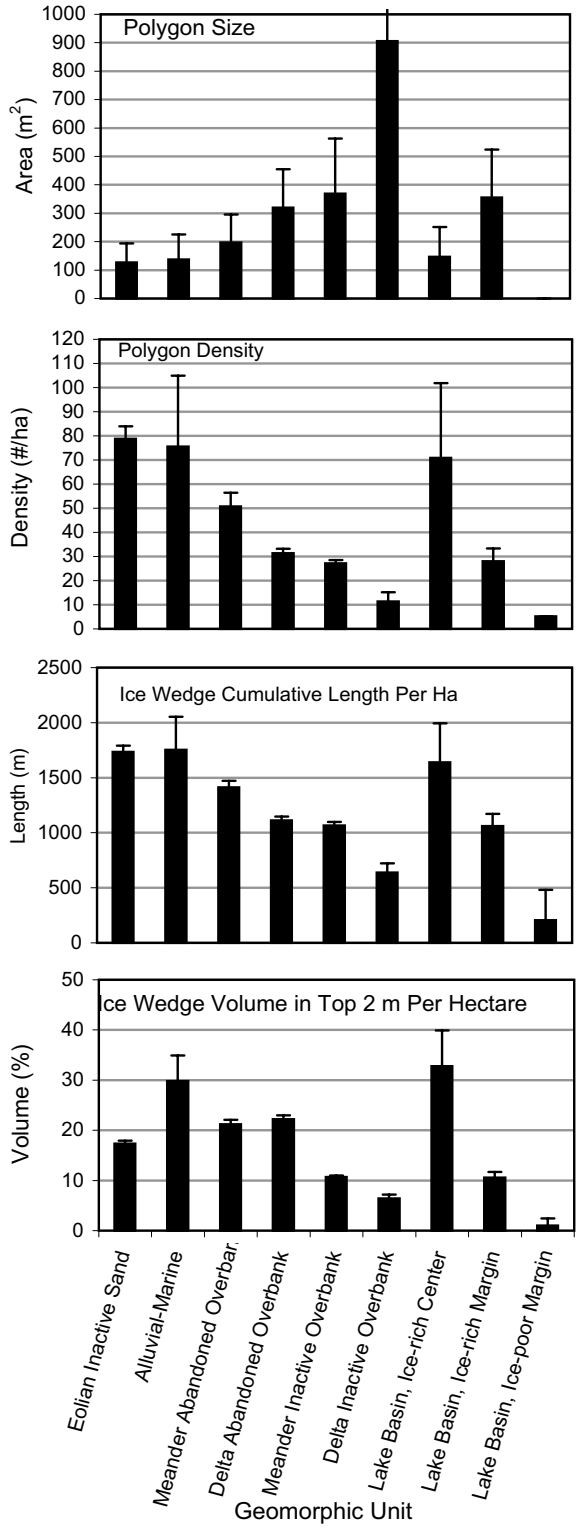

Figure 6. Mean size and density of ice-wedge polygons, cumulative length of ice wedges per hectare, and the percent volume of wedge ice in the top 2 m of permafrost by geomorphic unit, Northeast Planning Area, NPRA, 2004.

the permafrost ranged from 1% in ice-poor margins of lake basins to 33% in the ice-rich centers of lake basins (Figure 6). Abandoned overbank deposits (both delta and meandering) had twice as much wedge ice as inactive overbank deposits. Note that the pattern of ice volume in relation to terrain units differs somewhat from the trends in polygon size and density, because of the differing widths of the wedges.

We attribute the large differences in ice-wedge volume among terrain units to variation in both age and soil materials. The age of the terrain unit is important because a small amount of ice is added each year from seasonally cracking. Based on radiocarbon dating of basal peat, indicative of the age at which the mineral surface stabilized and ice wedges started growing (from Jorgenson et al. 1997, 2002), we estimate the age of the ice wedges to be: 5,000 to 8,000 years in alluvial-marine and eolian sand deposits; 3,000 to 5,000 years in ice-rich centers and margins of drained lake basins; 1,500 to 4,000 years in abandoned overbank deposits; 500 to 1,500 years in inactive overbank deposits; and 100 to 500 years in ice-poor margins of recently drained basins. In addition to growth in width, the density of ice-wedge polygons increases over time due to the subdivision of large polygons into smaller polygons, as is evident on inactive overbank deposits of intermediate age in Figure 5. Second, soils have that have accumulated thicker organic deposits or have more silt or clay, usually have higher segregated ice contents and contraction coefficients and, thus, are more easily deformed during ice-wedge formation. In contrast, ice-wedge development is much less in sandy or gravelly materials.

GROUND-PENETRATING RADAR

Subsurface imaging with a GPR along two long transects that crossed a variety of coastal plain deposits indicated the geophysical technique was useful for determining active-layer thickness, and to a lesser extent for delineating ice wedges and shallow sand deposits (Figures 7 and 8). A strong, continuous reflectance boundary with response times of 10–30 ns corresponded well with active-layer depths of 20–40 cm. The presence of ice wedges was differentiated by the low-amplitude responses within the 35–70 ns response time interval, and often by the shallow

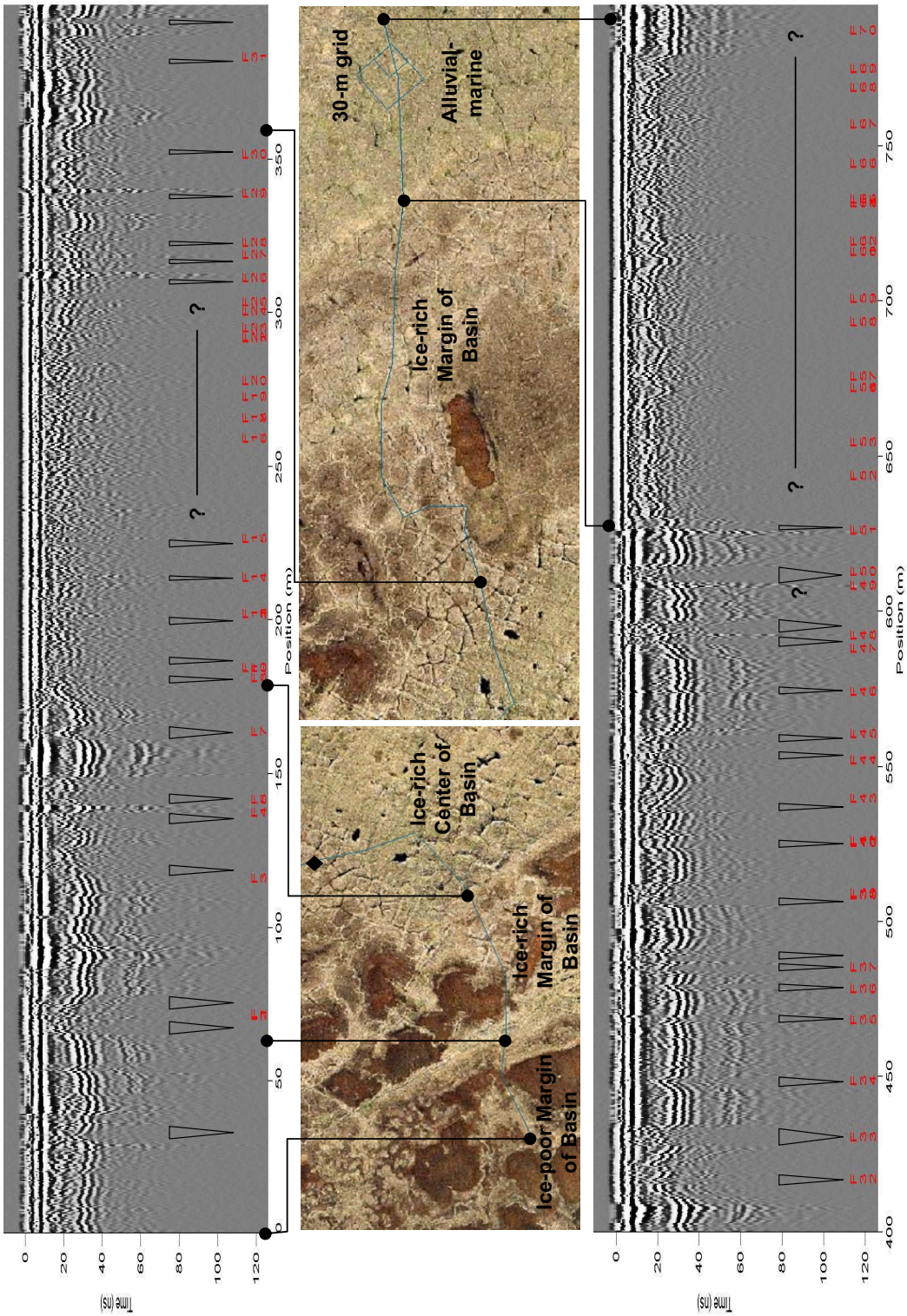

Figure 7. Ground-penetrating radar images for an 800-m transect near T1 in the Northeast Planning Area, NPRA, 2004. The cross-section illustrates the amplitudes of reflected microwaves for various time intervals related to depth (100 ns interval represents ~1.5 m depth). Terrain units are labeled on the photo. The triangles represent wedge locations interpreted from the images, the red "F" labels denote locations where wedges were observed on the ground, and the "?" denote locations where wedges were observed on the ground but not evident on the images.

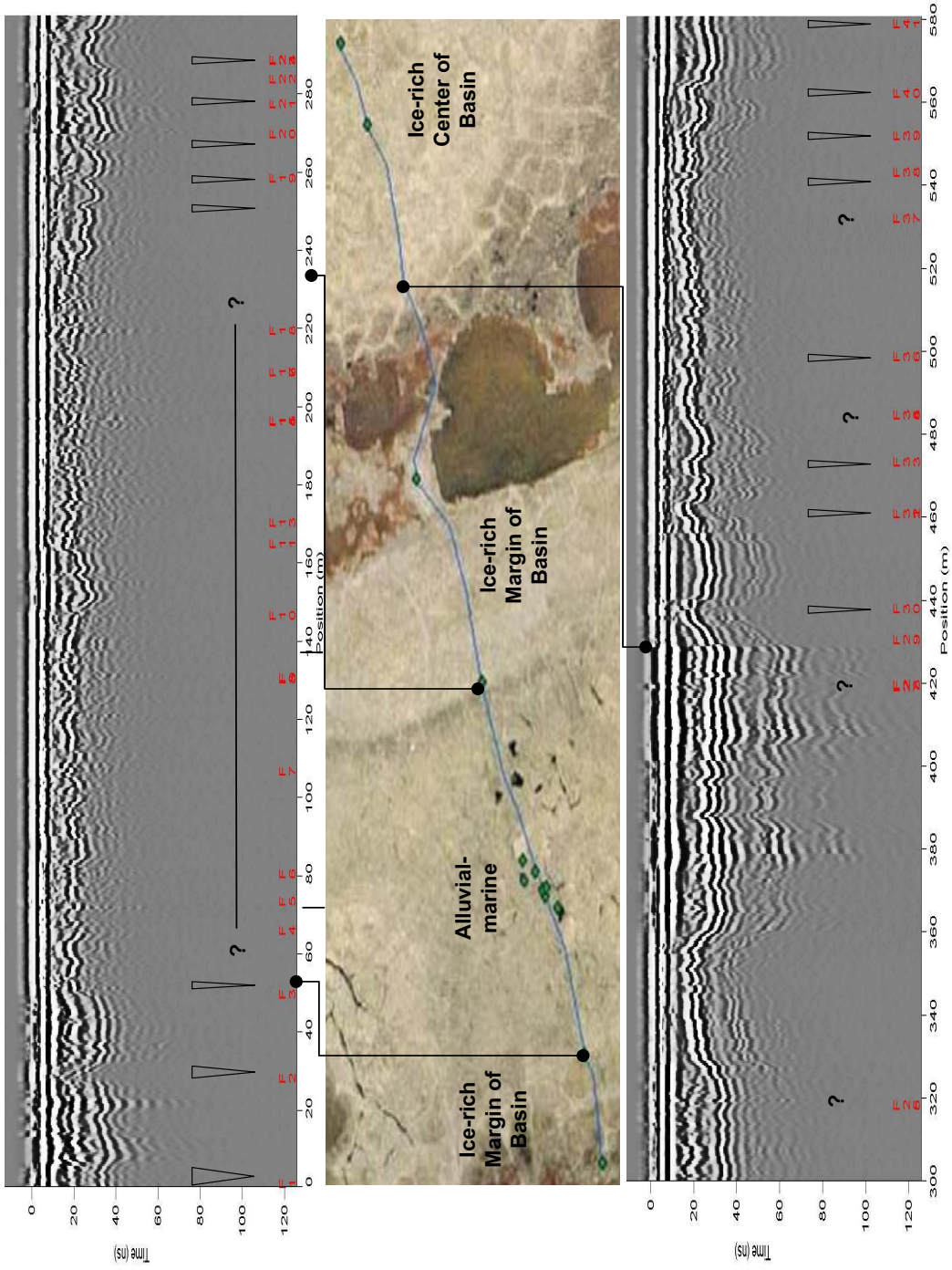

Figure 8. Ground-penetrating radar images for a 580-m transect near T11 in the Northeast Planning Area, NPRA, 2004. The cross-section illustrates the amplitudes of reflected microwaves for various time intervals related to depth (100 ns interval represents ~1.5 m depth). Terrain units are labeled on the photo. The triangles represent wedge locations interpreted from the images, the red "F" labels denote locations where wedges were observed on the ground, and the "?" denote locations where wedges were observed on the ground but not evident on the images.

active layers, or strong reflectance "humps," at the 20 ns response time. We attribute the low-amplitude reflectivity of the ice at depth to the reflection of energy at the surface of the ice wedge/permafrost and reduction of energy at depth, to higher signal velocities in ice, and to lack of discontinuities in the ice. The presence of sand was indicated by a high-amplitude reflectance in the 40–100 ns response-time interval. Although ice was strongly differentiated from sand, we suspect ice was poorly differentiated from peat and organic-rich loams due to the high ice contents of the organic-rich material. Consequently, the overlap in response characteristics between ice-rich materials makes it difficult to reliably identify the distribution of ice wedges along the entire transect. We estimate that the 100 ns response time corresponds with the ~1.5 m depth based on locations where we measured active-layer depths, although the time–depth relationship appears to vary with soil materials.

The GPR images also revealed differences in soil stratigraphy among the various terrain units. Alluvial-marine deposits had shallow active-layer depths and poorly differentiated subsurface materials, presumably due to the 12 m thick surface deposits of peat and organic-rich loam. The presence of tussock tundra on these older, raised deposits probably contributed to the poor differentiation because the tussocks raised and tilted the GPR cart as it was dragged along the ground, causing inconsistent signal direction and intensity. The ice-rich centers of basins also had poorly contracting signals, presumably due to the ice- and organic-rich silts that are typically >2 m deep. In contrast, ice-rich margins of drained basins had strong, continuous reflected signals from the permafrost table, consistently greater active-layer depths with frequent "humps" indicative of a shallow active layer, distinct ice wedges beneath the shallow active layer locations, and frequent high-amplitude responses from lacustrine sand deposits at depth. Ice-poor margins were similar except that the active layer was fairly uniform and ice wedges were uncommon.

GPR surveys along the 30-m and 15-m grids at T1, situated on an alluvial-marine deposit, revealed similar patterns but much stronger differentiation of soil materials (Figures 9 and 10). We interpreted the highest amplitudes to indicate sandy material at shallow depths, while the lowest amplitudes corresponded to ice wedges and ice-rich peat. When comparing grid maps created for the various time intervals, some interesting patterns are evident. At 12–20 ns (~18–30 cm depth), which encompasses the typical variation in the surface of the permafrost table, the lowest amplitudes (blue-purple) appear to correspond to areas with very shallow active-layer depths on higher microsites. At 25–40 ns (~35–60 cm), high-amplitude signals (yellow-red-white) indicate patches of shallow sand, while there was very little differentiation of the areas of ice wedges and ice-rich peat. At 60–80 ns (~90–120 cm), the lowest-amplitude signals appear to correspond to ice wedges, although ice-rich peats probably confuse the delineation. At 80–100 ns (~120–150 cm), the reflected signals are very weak, although sandy material is still somewhat differentiated. The best time-interval for differentiating ice was 40–80 ns (60–120 cm), which also corresponds to the depth at which ice wedges are widest (Figure 3). Note that signal amplitudes decrease rapidly with depth so the amplitude scale differs for each time interval. Locations of the ice wedges along one survey line are noted on both the grid map and the depth cross-section.

The accuracy of GPR for differentiating ice wedges was checked by coring at eight locations (Figure 10). The results of the coring indicated that there was a relatively good correspondence between earth materials and signal amplitude in the 35–70 ns time interval. For the three locations (black circles on Figure 10) where the amplitude of the response signals was relatively low (0–3, purple-dark blue), wedge ice was present near the surface (20–26 cm). For three locations (gray circles) with intermediate amplitude (3–7, light blue to green), wedge ice was found at intermediate depths (46–57 cm). For two sites (open circles) with relatively high amplitudes (6–9), sand was found at shallow depths and wedge ice was absent in the cores (> 120 cm depth). No cores were obtained from locations with very high amplitudes. The percent of the area that had low amplitudes (purple-dark blue) was 31%, indicating wedge ice occupied 31% of the ground volume at a depth of about 1 m. This value was the same as the percent volume for alluvial-marine deposits (31%) estimated by photointerpretation of ice wedge

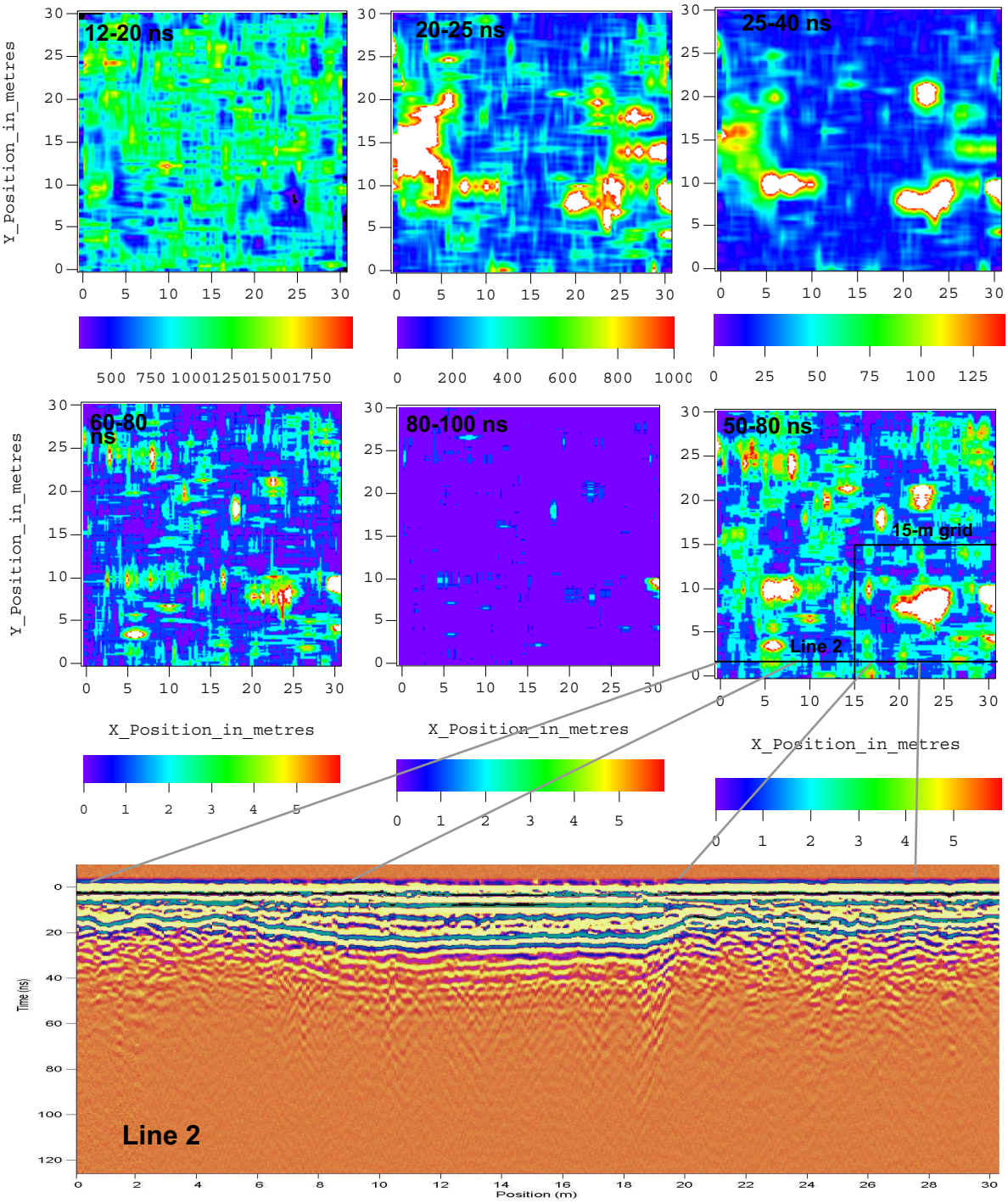

Figure 9. Ground-penetrating radar images for a 30-m grid near T1 in Northeast Planning Area, NPRA, 2004. The grid maps illustrate amplitude of reflected microwaves for various time intervals related to depth (100 ns interval represents ~1.5 m depth) and amplitude scale changes with depth. The cross-section profile is along line two. The cores are labeled by their active-layer depth.

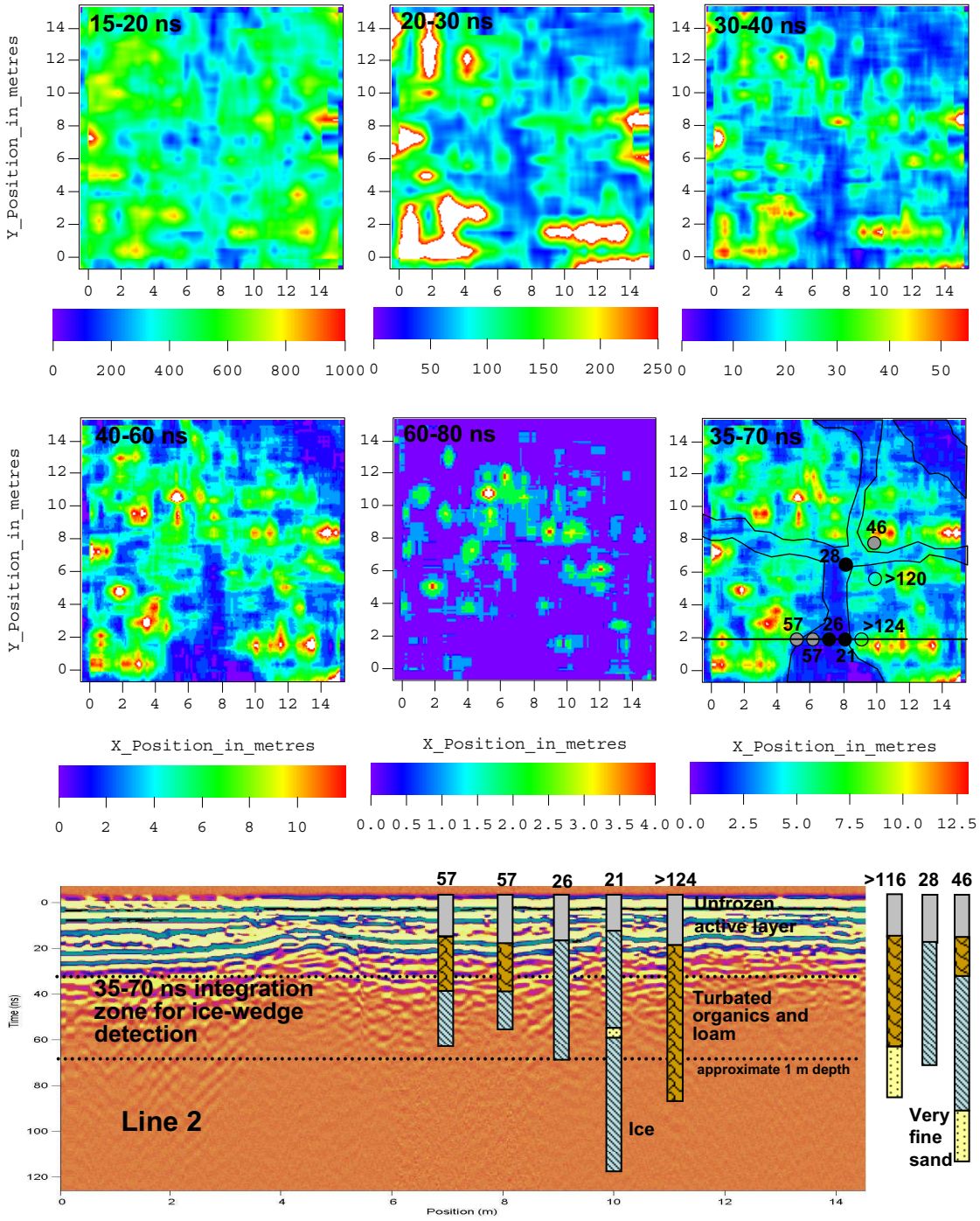

Figure 10. Ground-penetrating radar map for a 15-m grid near T1 in the Northeast Planning Area, NPRA, 2004. The grid maps illustrate amplitude of reflected microwaves for various time intervals related to depth (100 ns interval represents ~1.5 m depth) and amplitude scale changes with depth. The cross-section profile is along line two.

distribution. Although these samples indicate fairly good correlation between amplitude and earth materials, the sample size was small. More testing across the entire range of amplitudes is needed to accurately assess the reliability of GPR for imaging subsurface earth materials. In any survey using GPR, some soil coring will always be needed to help guide the interpretation of the images.

DISCUSSION

Field descriptions of exposed ice wedges revealed more complexity in the development and deformation of ice wedges than has previously been recognized in the scientific literature. Although the mechanisms of seasonal contraction cracking, the deformation of adjacent soils, and creation of soil ridges have long been recognized (Leffingwell 1919, Lachenbruch 1962, Péwé 1975), the complex processes affecting ice-wedge evolution have been inadequately investigated. This study has contributed to the growing body of information on ice wedges by identifying: (1) multiple levels at the top of many wedges indicative of multiple episodes of degradation and aggradation, as well as rounded upper surfaces from very gradual active-layer adjustment; (2) the presence of congelation ice that has developed in surface and lateral cavities in the ice wedges from degradation by water and subsequent refreezing; (3) the failure and cracking of large wedges from compressive forces; and (4) complex deformation structures in adjacent soils that include vertical squeezing and extrusion of soil masses, down-turning of soil layers as well as up-turning.

The photogrammetric analysis of ice-wedge abundance and distribution also revealed more variation than previously described. Studies of ice-wedge abundance are few (Leffingwell 1919, Brown 1968, Pollard and French 1980) and generally have estimated that ice wedges occupy 10–20% of the volume of the ground near the surface. We found, however, that ice-wedge volume was highly variable and that the variability could be related to terrain units of differing soil materials, genesis, and age. Of particular interest are the very high ice volumes found in alluvial-marine deposits and delta abandoned overbank deposits, both of which have thick organic accumulations and fine-grained soils, and are among the oldest deposits.

The testing of GPR for imaging subsurface soils along transects revealed that the ability of this technique to detect ice wedges varied by terrain type. For terrain units with sandy soils and low organic contents (e.g., ice-poor margins of lake basins), the ice wedges were readily differentiated from the surrounding soil. However, in terrain units with very thick ice-rich organic accumulations (e.g., alluvial-marine deposits), the ice wedges were poorly differentiated in the images, particularly in cross-section view. Grid surveys showed better potential for mapping ice wedges because the 3-D averaging of signal amplitude reduces noise and thus allows better differentiation of soil materials. Assuming that the dark signatures (blue and purple) represent wedge ice, the volume of ice determined by GPP is 31%. This is similar to the 31% determined to be the mean volume of ice as determined from photogrammetry and ice wedge cross-sections. Both transect and grid surveys, however, were ineffective at imaging the geometry of ice wedges and thus seriously limits the confidence in ice-wedge volumes determined with GPR.

Overall, the assessment of GPR data is mixed. Photointerpretation of ice-wedge distribution based on surface microtopography is easier and much faster than GPR surveys. GPR surveys may be advantageous in hilly terrain, however, where surface microtopography from ice wedges is eliminated by slope mass-wasting processes, rendering photointerpretation difficult. GPR surveys also have the advantage of recording active-layer depths and to a lesser extent differentiating the stratigraphy of soils with distinctly differing lithologies.

The large variation in ice-wedge volume among terrain units has important implications for assessing terrain sensitivity and planning land rehabilitation. Previous studies have found that ice-wedges are very sensitive to surface disturbance and climatic changes (Burn 1990, Jorgenson et al. 2003). Therefore, the volume of ice is an important factor affecting how easily thermokarst can be initiated and how extensively it will develop. Both alluvial marine deposits and the ice-rich centers of lake basins have very high

ice-wedge volumes (~30%) and thus are very sensitive to disturbance. This is evident in the abundance of high-centered polygon microtopography on both terrain types and the occurrence of thermokarst lakes that are eroding into ice-rich centers of lake basins. The sensitivity of ice-wedges to disturbance also is evident in the prevalence of polygonal thermokarst development adjacent to heavily used roads in the Prudhoe Bay oilfield. Improved understanding of ice-wedge distribution and abundance can now be used to improve the conceptual models of the responses of terrain to disturbance and the predictions of the microtopography that is likely to result during land rehabilitation (Jorgenson et al. 2002).

Application of improved information on ice-wedge abundance and distribution remains problematic for facility siting, however, because of the trade offs in multiple environmental concerns. For example, during facility planning for oil development in the NPRA, roads and pads were preferentially sited along the crests of upland ridges to avoid hydrologic cross-drainage issues and high-value habitat in lake basins, even though the alluvial-marine deposits that form these ridges are very ice-rich. In contrast, the ice-rich centers of lake basins were successfully avoided. Based on the development of conceptual models of permafrost response to disturbance that have been developed using this information (Jorgenson et al. 2002), the isolated patches of thermokarst that are expected to occur near the road are not likely to propagate very far, due to the polygonal pattern of thermokarst development and the ability of ice-wedges to stabilize after minor disturbance.

SUMMARY AND CONCLUSIONS

Permafrost greatly influences the engineering properties of the soil, ecosystem development, and the response of the terrain to human activities. Accordingly, the study of terrain relationships for predicting the nature and distribution of ground ice across the landscape, and the ability to predict the response of permafrost to disturbance are essential to assessing potential impacts from oil development in the National Petroleum Reserve–Alaska (NPRA). This fourth year of permafrost studies in northeastern NPRA focused on the study of ice wedges, which have the highest sensitivity to disturbance. Objectives of this study were to: (1) describe the morphological characteristics of ice wedges; (2) estimate the abundance and distribution of ice wedges in various terrain units, and (3) assess the use of ground-penetrating radar (GPR) for mapping ice-wedge distribution.

Examination of 24 exposed ice wedges along Fish Creek revealed wide variability in both dimensions and ice characteristics. The mean width of the 12 ice wedges that had transverse exposures increased from 1.3 m at the top to a maximum of 1.9 m at the 1-m depth from the wedge top, then slowly decreased to 1.2 m at 2-m depth and 0.6 m at the 3-m depth. Maximum widths of ~3 m were common. Factors that lead to complex morphology of the ice wedges, included: (1) multiple levels of the surface boundary indicating multiple episodes of degradation and aggradation, as well as rounded upper surfaces from very gradual active-layer adjustment; (2) the presence of congelation ice that has developed in surface and lateral cavities in the ice wedges from degradation by water and subsequent refreezing; (3) the failure and cracking of large wedges from the compressive forces; and (4) complex deformation structures that included vertical squeezing and extrusion of soil masses, and up-turning and down-turning of soil layers.

The mapping of ice wedges through photointerpretation of high-resolution aerial photography revealed large differences in the abundance and distribution of ice wedges among terrain units. The mean percent volumes of wedge ice in the top 2 m of permafrost was highest in alluvial-marine deposits (31%) and ice-rich centers of lake basins (33%). Mean percent volumes in delta abandoned overbank deposits (22%) and meander abandoned overbank deposits (21%) was two to three times higher than in delta inactive overbank deposits (6%) and meander inactive overbank deposits (11%). Ice-wedge volume was much higher in the ice-rich margins of lake basins (11%), than in the ice-poor margins of lake basins (1%). We attribute the large differences in ice-wedge volume to both age and soil materials.

Subsurface imaging with a GPR along two long transects and two small grids situated on a variety of coastal plain deposits indicated the geophysical technique was useful for determining

active-layer thickness, and to a lesser extent for delineating ice wedges and shallow sand deposits. The GPR images also revealed differences in soil stratigraphy among the various terrain units. Ice wedges were readily differentiated in terrain units with sandy soils and low organic contents (e.g. ice-rich margins of lake basins), and poorly differentiated in terrain units with thick ice-rich organic accumulations (e.g. alluvial-marine deposits). Three-dimensional imaging along grids showed better differentiation of ice-wedges and soil materials than did the 2-D transects. The percent volumes of ice wedges in alluvial-marine deposits estimated through GPR (31%) and photointerpretated maps (31%) were similar.

The large variation in ice-wedge volume among terrain units has important applications for assessing terrain sensitivity and for land rehabilitation planning. Because ice-wedges are very sensitive to surface disturbance and climatic changes, the volume of wedge ice is an important factor in how easily thermokarst can be initiated and the extent to which thermokarst will develop. Accordingly, knowledge of the variability in abundance and distribution ice wedge is useful for avoiding sensitive terrain during facility planning, although not all ice-rich terrain can be avoided during exploration and development because surface hydrology, habitat, and wildlife issues are also prominent considerations. The information also can be used to improve upon existing conceptual models of the response of terrain to disturbance and to predict of the microtopography that is likely to result during land rehabilitation.

LITERATURE CITED

Annan, A. P., and J. L. Davis. 1976. Impulse radar sounding in permafrost. Radio Science 2:383–394.

Arcone, S. A., and A. J. Delaney. 1982. Dielectric properties of thawed active layers overlying permafrost using radar at VHF. Radio Science 17:618–626.

Arcone, S. A., P. V. Sellmann, and A. J. Delaney. 1982. Radar Detection of Ice Wedges in Alaska. U.S. Army Cold Regions Research and Engineering Laboratory, Hanover, NH. CRREL Rep. 82–43. 15 p.

Billings, W. D., and K. M. Peterson. 1980. Vegetational change and ice-wedge polygons through the thaw lake cycle in Arctic Alaska. Arctic and Alpine Research 12: 413–432.

Britton, M. E. 1957. Vegetation of the Arctic tundra. Pages 67–113 *in* H. P. Hansen, ed. Arctic Biology: 18th Biology Colloquium. Oregon State University Press, Corvallis.

Brown, J. 1968. An estimation of the volume of ground ice, Coastal Plain, Northern Alaska. U. S. Army Cold Regions Research and Engineering Laboratory, Hanover, NH.

Brown, J., and N. A. Grave. 1979. Physical and thermal disturbance and protection of permafrost. U.S. Army Cold Regions Research and Engineering Laboratory, Hanover, NH. Special Rep. 79–5. 42 pp.

Burgess, R. M., E. R. Pullman, and M. T. Jorgenson. 1998. Evaluation of vertical migration of salts from buried reserve pit materials in the Kuparuk and Prudhoe Bay oilfields. Final report prepared for Arco Alaska, Inc., Anchorage, by ABR, Inc., Fairbanks, AK. 55 pp.

Burgess, R. M., E. R. Pullman, T. C. Cater, and M. T. Jorgenson. 1999. Rehabilitation of salt-affected land after close-out of reserve pits. Third Annual Report prepared for ARCO Alaska, Inc., Anchorage, AK, by ABR, Inc., Fairbanks, AK. 48 pp.

Burn, C. R. 1990. Implications for palaeoenvironmental reconstruction of recent ice-wedge development at Mayo, Yukon Territory. Permafrost and Periglacial Processes 1(1):3–14.

Carter, L. D., J. A. Heginbottom, and M. Woo. 1987. Arctic Lowlands. Pages 583–628 *in* Geomorphic Systems of North America. Centennial Special Volume, 2 ed., U.S. Geological Society of America, Boulder, CO.

Doolittle, J. A., M. A. Hardisky, and S. Black. 1990. A ground-penetrating radar study of active layer thicknesses in areas of moist sedge and wet sedge tundra near Bethel, Alaska, U.S.A. Arctic and Alpine Research 22:175–182.

Emers, M., and J. C. Jorgenson. 1997. Effects of winter seismic exploration on tundra vegetation and the soil thermal regime on the Arctic National Wildlife Refuge, Alaska. Pages 443–456 *in* R. M. M. Crawford, ed. Disturbance and Recovery in Arctic Lands, An Ecological Perspective. Kluwer Academic Publishers, Dordrecht, Netherlands.

Entrix. 2004. Alpine Satellite Development Plan EIS. Report for U.S. Bureau of Land Management, Anchorage, AK by Entrix, Inc., Anchorage, AK.

Fortier, D., and M. Allard. 2004. Late Holocene syngenetic ice-wedge polygons development, Bylot Island, Canadian Arctic Archipelago. Canadian Journal of Earth Science 41:997–1012.

Hinkel, K. M., J. A. Doolittle, J. G. Bockheim, F. E. Nelson, R. Paetzold, J. M. Kimble, and R. Travis. 2001. Detection of subsurface permafrost features with ground-penetrating radar, Barrow, Alaska. Permafrost and Periglacial Processes 12:179–190.

Johnson, G. H. 1981. Permafrost Engineering Design and Construction. National Research Council of Canada, Ottawa, Canada. 540 pp.

Jorgenson, M. T. 1986. Biophysical factors affecting the geographic variability of soil heat flux. M.S. Thesis, Univ. of Alaska, Fairbanks, 109 pp.

Jorgenson, M. T., and J. G. Kidd. 1991. Land rehabilitation studies in the Prudhoe Bay Oilfield, Alaska, 1990. Annual report prepared for ARCO Alaska, Inc., Anchorage, AK, by Alaska Biological Research, Inc., Fairbanks, AK. 57 pp.

Jorgenson, M. T., T. C. Cater, M. Joyce, and S. Ronzio. 1992. Cleanup and bioremediation of a crude-oil spill at Prudhoe Bay, Alaska. Pages 715–722 *in* Proceedings of the Fifteenth Arctic and Marine Oil Spill Program Technical Seminar. Edmonton, Alberta. Environment Canada, Ottawa, Ontario.

Jorgenson, M. T., L. W. Krizan, and M. R. Joyce. 1991. Bioremediation and tundra restoration after an oil spill in the Kuparuk Oilfield, Alaska, 1990. Pages 149–154 *in* Proceedings of the 14th Annual Arctic and Marine Oil Spill Technical Program. Environ. Canada, Ottawa, ON.

Jorgenson, M. T., E. R. Pullman, T. Zimmer, Y. Shur, A. A. Stickney, and S. Li. 1997a. Geomorphology and hydrology of the Colville River Delta, Alaska, 1996. Final report prepared for ARCO Alaska, Inc., Anchorage, AK, by ABR, Inc., Fairbanks, AK. 148 pp.

Jorgenson, M. T., Y. Shur, and H. J. Walker. 1998. Factors affecting evolution of a permafrost dominated landscape on the Colville River Delta, northern Alaska. Pages 523–530 *in* A. G. Lewkowicz, and M. Allard, eds. Proceedings of Seventh International Permafrost Conference. Universite Laval, Sainte-Foy, Quebec. Collection Nordicana, No. 57.

Jorgenson, M. T., E. R. Pullman, and Y. Shur. 2002. Geomorphology of the NPRA study area, northern Alaska. First Annual Report prepared for Phillips Alaska, Inc., Anchorage, AK, by ABR, Inc., Fairbanks, AK. 50 pp.

Jorgenson, M. T., E. R. Pullman, and Y. L. Shur. 2003a. Geomorphology of the Northeast Planning Area of the National Petroleum Reserve-Alaska, 2002. Second Annual Report prepared for Phillips Alaska, Inc., Anchorage, AK, by ABR, Inc., Fairbanks, AK. 67 pp.Jorgenson, M. T., J. E. Roth, M. Emers, S. Schlentner, and J. Mitchell. 2003. Assessment of ecological impacts associated with seismic exploration near the Colville Delta . Pages 7 (abstract) *in* Alaska Conference on Reducing the Effects of Oil and Gas Exploration and

Production on Alaska's North Slope: Issues, Practices, and Technologies. Idaho National Engineering and Environmental Laboratory, Department of Energy.

Jorgenson, M. T., E. R. Pullman, and Y. L. Shur. 2004. Geomorphology of the Northeast Planning Area of the National Petroleum Reserve-Alaska, 2003. Third Annual Report prepared for ConocoPhillips Alaska, Inc., Anchorage, AK, by ABR, Inc., Fairbanks, AK. 40 pp.

Kidd, J. G., L. L. Jacobs, T. C. Cater, and M. T. Jorgenson. 1997. Ecological restoration of the North Prudhoe Bay State No, 2 exploratory drill site, Prudhoe Bay Oilfield, Alaska, 1995. Final Report prepared for ARCO Alaska, Inc., Anchorage, AK, by ABR, Inc., Fairbanks, AK. 36 pp.

Kidd, J. G., B. Streever, M. R. Joyce, and L. H. Fanter. 2004. Wetland restoration of an exploratory well on Alaska's North Slope: a learning experience. Ecological Restoration 22:30–38.

Kovacs, A., and R. M. Morey. 1985. Impulse radar sounding of frozen ground. Pages 28–40 *in* Workshop on Permafrost Geophysics, Golden, Colorado, Oct. 23-24, 1984. U.S. Army Cold Regions Research and Engineering Laboratory, Hanover, NH. CRREL Special Report 85-5.

Kreig, R. A., and R. D. Reger. 1982. Air-photo analysis and summary of landform soil properties along the route of the Trans-Alaska Pipeline System. Alaska Division of Geological and Geophysical Surveys, Fairbanks, AK. Geologic Report 66. 149 pp.

Lachenbruch, A. H. 1962. Mechanics of thermal contraction cracks and ice-wedge polygons in permafrost. Geological Society of America, Special Paper 70. 69 pp.

Lawson, D. E. 1986. Response of permafrost terrain to disturbance: a synthesis of observations from northern Alaska, U.S.A. Arctic and Alpine Research 18:1–17.

Leffingwell, E. de K. 1919. The Canning River region of northern Alaska. U.S. Government Printing Office, Washington, D.C. U.S. Geological Survey Professional Paper 109. 251 pp.

Leffingwell, E. de K. 1915. Ground-ice wedges, the dominant form of ground-ice on the north coast of Alaska. Journal of Geology 23:635–654.

Mackay, J. R. 1992. The frequency of ice-wedge cracking (1967–1987) at Garry Island, western Arctic coast, Canada. Canadian Journal of Earth Sciences 30:1720–1729.

McFadden, T. T., and F. L. Bennet. 1991. Construction in Cold Regions—A Guide for Planners, Engineers, Contractors, and Managers. John Wiley and Sons, Inc., New York, NY.

Parametrix, Inc. 1997. Alpine development project environmental evaluation document. Report for ARCO Alaska, Inc. by Parametrix, Inc., Kirkland, WA.

Péwé, T. L. 1966. Ice wedges in Alaska; classification, distribution, and climatic significance. Pages 76–81 *in* Proceedings, Permafrost, International Conference. National Academy of Sciences, Washington, D.C.

Péwé, T. L. 1975. Quaternary geology of Alaska. U.S. Geological Survey, Geol. Surv. Prof. Pap. 835. 145 p.

Pilon, J. A., A. P. Annan, and J. L. Davis. 1985. Monitoring permafrost ground conditions with ground probing radar (G. P. R.). Pages 71–73 *in* Workshop on Permafrost Geophysics, Golden, Colorado, Oct. 23–24, 1984. U.S. Army Cold Regions Research and Engineering Laboratory, Hanover, NH. CRREL Special Report 85-5.

Pollard, W. H., and H. M. French. 1980. A first approximation of the volume of ground ice, Richards Island, Pleistocene Mackenzie Delta, Northwest Territories, Canada. Canadian Journal of Earth Sciences 17:509–516.

Pullman, E. R., M. T. Jorgenson, T. C. Cater, W. A. Davis, and J. E. Roth. 2005. Assessment Of Ecological Effects Of The 20022003Ice Road Demonstration Project. Final Reports prepared for ConocoPhillips Alaska, Inc., Anchorage, AK, by ABR, Inc., Faibanks, AK.

Scott, W. J., P. V. Sellmann, and J. A. Hunter. 1990. Geophysics in the study of permafrost. Pages 355–384 *in* S. H. Ward, ed., Geotechnical and Environmental Geophysics. Society of Exploration Geophysicists.

Walker, D. A., K. R. Everett, P. J. Webber, and J. Brown. 1980. Geobotanical atlas of the Prudhoe Bay region, Alaska. U.S. Army Corps of Engineers Cold Regions Research and Engineering, Hanover, NH. Laboratory Report 80-14. 69 p.

Walker, D. A. 1981. The vegetation and environmental gradients of the Prudhoe Bay region, Alaska. Unpublished report by University of Colorado, Boulder.

Walker, D. A., D. Cate, J. Brown, and C. Racine. 1987. Disturbance and recovery of arctic Alaskan tundra terrain: a review of investigations. U.S. Army Cold Regions Research and Engineering Laboratory, Hanover, NH. CRREL Rep. 87-11.

Webber, P. J., and J. D. Ives. 1978. Damage and recovery of tundra vegetation. Environmental Conservation 5: 171–182.

Webber, P. J., P. C. Miller., F. S. Chapin III, and B. H. McCown. 1980. The vegetation: pattern and succession. Pages 186–218 *in* J. Brown, P. C. Miller, L. L. Tieszen, and F. L. Bunnell, eds. An arctic ecosystem, the coastal tundra at Barrow, Alaska. Dowden, Hutchinson, and Ross, Stroudsburg, PA.